Ionic silver coating of orthopedic implants may impair osteogenic differentiation and mineralization

MICHAEL G. KONTAKIS, ELIN CARLSSON, CARLOS PALO-NIETO and NILS P. HAILER

OrthoLab, The Rudbeck Laboratory, Department of Surgical Sciences/Orthopedics, Uppsala University, 75185 Uppsala, Sweden

Received October 4, 2024; Accepted December 6, 2024

DOI: 10.3892/etm.2025.12801

Abstract. Silver (Ag) possesses potent antimicrobial properties and is used as a coating for medical devices. The impact of silver ions released from orthopedic implants on the differentiation and osteoid formation of different osteogenic cells has yet to be systematically studied. In the present study, human mesenchymal stem cells (hMSCs) and primary human osteoblasts (hOBs) were exposed to different static Ag^+ concentrations (0, 0.5, 1.0 or 1.5 ppm) or dynamic Ag^+ concentrations (range 0 to 0.7 ppm) that simulated the temporal release pattern from a Ag-nitrate coating of trabecular titanium (TLSN). Cell morphology was investigated by phase contrast and fluorescence microscopy. The activities of alkaline phosphatase (ALP) and lactate dehydrogenase, osteogenic gene expression (COL1A1, COL1A2 and ALPL), and osteoid deposition were examined for up to 4 weeks. DAPI and carboxyfluorescein diacetate staining revealed changes in the morphology of hOBs treated with ≥0.5 ppm Ag^+, while osteocalcin-positive cells were observed primarily in the untreated group. Elevated Ag^+ concentrations did not impact the production of ALP by either hMSCs or hOBs. Treatment with 1.5 ppm Ag^+ or TLSN Ag^+ led to a modest reduction in COL1A2 and ALPL levels in hMSCs at 2 weeks but not at 4 weeks nor in hOBs. In hMSC cultures, mineralization decreased at ≥1 ppm Ag^+, whereas the same concentration range significantly reduced mineralization in hOB cultures. In conclusion, Ag^+ concentrations ranging from 1.0 to 1.5 ppm may interfere with osteogenic differentiation, possibly by altering gene expression, thereby affecting mineralization. Only Ag^+ concentrations up to 0.5 ppm allowed undisturbed osteogenic differentiation and mineralization. These findings pertain to creating Ag coatings of titanium intended for cementless fixation into host bone.

Correspondence to: Mr. Michael G. Kontakis, OrthoLab, The Rudbeck Laboratory, Department of Surgical Sciences/Orthopedics, Uppsala University, C11 Ground Floor, 20 Dag Hammarskjölds väg, 75185 Uppsala, Sweden
E-mail: mikael.kontakis@uu.se

Key words: silver-coating, osseointegration, human osteoblasts, infection

Introduction

Silver (Ag) can be used as a coating for orthopedic implants due to its antimicrobial properties (1), with applications primarily in arthroplasty in tumor patients (2) and in revisions performed due to periprosthetic joint infections (3). Ionic silver (Ag^+) exerts numerous intracellular effects, including opening of pores in the bacterial membrane, denaturation of intracellular proteins, and accumulation of DNA damage caused by the generation of reactive oxygen species (4). Similarly, Ag^+ poses potential toxicity to osteogenic cells (5,6). This is why Ag-coated implants are not used clinically for cementless fixation of arthroplasty implants: coatings are limited to their extraosseous components only. An exception to this is the Kyocera® Ag-hydroxyapatite coating, which is applied to cementless cups, stems, and lumbar interbody cages (7,8).

Several orthopedic implants equipped with Ag coatings are currently in clinical practice. These include the electrochemically Ag-coated MUTARS® prosthesis (Implantcast), containing 0.7-1.2 grams of Ag per implant, and hip or knee megaprostheses with a thinner PorAg® coating deposited by physical vapor deposition (Waldemar Link), containing up to 0.33 grams per implant. The Agluna® implants intended for primary arthroplasty are electrochemically coated with only 0.006 g of Ag per implant (3,9), whereas the Kyocera® implants have 0.0028 g of Ag per implant (8). Ag^+ levels in the blood of patients who have received these prostheses range from 1.4 to 200 ppb (9), and the reported side effects (e.g., local argyria) are generally mild and rare (10-12). Ag-coated intramedullary nails with covalently attached Ag on the titanium surface of the nail (Bactiguard®) have been used in open long bone fractures (13), leading to uneventful bone healing with few infections. Plates for fracture fixation have also been coated with Ag (14). Although Ag-coated locking plates are still not commonplace in clinical practice, evidence from a rabbit humerus osteotomy model showed uneventful fracture healing when bridged with an Ag-coated plate containing 60 μg of Ag (15). The PorAg® coating, commonly used in oncological cases and periprosthetic joint infections, reduces bacterial counts by 68% compared to uncoated, grit-blasted titanium. This benefit, however, is offset by a reduction in osteoblast viability (5).

Ag-mediated toxicity to osteogenic cells is dose dependent (16). Therefore, below a specific concentration threshold, the osteoconductivity of the implant should not be hampered

while sufficient antibacterial activity is maintained. Our previous research showed that additively manufactured trabecular titanium coated with silver nitrate (TLSN) containing 7 at% of Ag effectively suppressed *S. aureus* biofilm formation. Conversely, the alkaline phosphatase (ALP) and lactate dehydrogenase (LDH) activity of osteoblasts cultured on these samples did not differ from that of osteoblasts cultured on uncoated titanium (6).

The literature concerning the effects of Ag^+ concentrations on the gene expression profile of osteogenic markers, bone differentiation, and mineralization of human osteogenic cells and primary human osteoblasts is sparse. The genes encoding alkaline phosphatase (ALPL) and collagen type I chains a1 and a2 (COL1A1 and COL1A2) are early markers of osteogenic differentiation and defects in these genes are implicated in such diseases as hypophosphatasia and osteogenesis imperfecta (17,18). Osteocalcin (OCN) is a glycoprotein synthesized by osteoblasts at their later stages of differentiation, plays an important role in bone mineralization by binding calcium and hydroxyapatite (19-21). Therefore, the expression of the proteins mentioned above is a prerequisite for a healthy bone matrix, which is essential for osseointegration and long-term implant stability (22).

Consequently, this study sought to investigate the effects of elevated Ag^+ concentrations on titanium's osseointegration potential. We examined the impact of different Ag^+ concentrations on the morphology, osteogenic differentiation, expression of the ALPL, COL1A1, and COL1A2 genes, and mineralization by human mesenchymal stem cells (hMSCs) and primary human osteoblasts (hOBs).

Materials and methods

Cells and culture. hMSCs derived from bone marrow were purchased from Sigma (C-12974) and stored in liquid nitrogen until use. hOBs were collected from five different patients who underwent hip arthroplasty at Uppsala University Hospital between Q4 2022 and Q1 2024 (Swedish Ethical Review Authority approval number 2020-04462), using a previously published protocol (23). Briefly, the retrieved femoral heads were diced into small fragments, which were rinsed with PBS and then placed in 25-cm^2 flasks containing alpha-modified minimum essential medium (αMEM; Cytiva SH30265.01, obtained from Fisher Scientific 10346952), 10% fetal bovine serum (FBS; Sigma-Aldrich/Merck F9665), 1% penicillin/streptomycin, and 0.5% amphotericin B (Cytiva HyClone®, Fisher Scientific 11556461 and Gibco® 15290026, Fisher Scientific 11520496). The culture medium (5 ml) was refreshed once weekly until confluence was reached.

To investigate the effects of Ag^+ on cell viability and differentiation, different concentrations of $AgNO_3$ (Sigma-Aldrich/Merck S6506) were added to the culture media. Both hMSCs and hOBs used for immunohistochemistry and differentiation studies were cultured in αMEM supplemented with 10% FBS, 1% PeSt, and 0.5% amphotericin B for 4 weeks. $AgNO_3$ was introduced to the growth media at concentrations of 0 ppm (control), 0.5 ppm, 1 ppm, 1.5 ppm and at the dynamic concentration range of TLSN (Table I). This addition took place 24 h after cell seeding (day 0). The Ag^+ concentrations in Table I simulate the temporal release profile of Ag^+ from TLSN implants, as discussed previously (6). The cells were seeded in 24-well plates at a density of 35,000 cells per well, with cell numbers measured using a NucleoCounter®, and the medium (1 ml per well) was refreshed every other day. After 1 week of culture, the medium was supplemented with 10 mM β-glycerophosphate (Sigma-Aldrich/Merck G9422), 100 nM dexamethasone (Sigma-Aldrich/Merck D4902), and 80 μM ascorbic acid (Sigma-Aldrich/Merck A4544) to stimulate osteoblastic differentiation. Cell morphology and viability were examined at 3, 7, 14, 21, and 28 days using live-image microscopy (Leica DMi8 Microscope with INCUBATORi8 environmental chamber). Representative phase contrast images were taken at all time points (10x magnification, 12 ms exposure time).

Cell experiments with hMSCs and hOBs were performed in triplicates. For hOBs, four biological replicates (n=4) were used for ALP and LDH assays, two biological replicates for the gene experiments after 1 and 2 weeks, five biological replicates for the gene experiments after 4 weeks, and one biological replicate for the mineralization assay (Fig. S1).

Osteogenic differentiation. Osteogenic differentiation was expressed as the ratio between alkaline phosphatase (ALP) and lactate dehydrogenase (LDH) ALP/LDH, and was assessed after 1, 2, and 4 weeks of exposure to Ag^+. The medium was discarded, and the cells were rinsed with PBS, followed by enzymatic lysis with 400 μl of lysis buffer (CelLytic® M, Sigma-Aldrich/Merck C2978) per well for 15 min on a shaker at room temperature (RT). 50 μl of the lysate was mixed with the *In Vitro* Toxicology Assay Kit (LDH, TOX7; Sigma-Aldrich/Merck) and the ALP substrate (p-nitrophenyl phosphate; Sigma-Aldrich/Merck P7998) in 96-well plates, as per the manufacturer's protocol. The 96-well plates were incubated at 37˚C for 30 min, and the absorbance was measured in a spectrophotometer at 690 and 492 nm (Multiscan Ascent, ThermoFisher Scientific, Waltham, MA, USA) for LDH and at 405 nm for ALP. ALP absorbance values were converted to concentrations (in mM) using a standard calibration curve of nitrophenol dilutions (4-Nitrophenol solution, Sigma-Aldrich/Merck N7660) ranging from 0 to 2.5 mM.

COL1A1, COL1A2, and ALPL gene expression. The messenger RNA (mRNA) levels of osteogenic-related genes in hMSCs and hOBs were analyzed through real-time quantitative polymerase chain reaction (RT-qPCR) at 1, 2, and 4 weeks. The cells were cultured as previously described, lysed at the endpoints using 400 μl of TRIzol® (Invitrogen®, bought from ThermoFisher 15596026) and stored at -20˚C until use. Ribonucleic acid (RNA) extraction was performed according to the manufacturer's protocol, and the total RNA yield was determined using a Nanodrop (ND-1000 Spectrophotometer, ThermoFisher Scientific Inc., Waltham, MA, USA). Subsequently, RNA was reverse transcribed into complementary DNA (cDNA) (High Capacity RNA to c-DNA® kit, Applied Biosystems®, bought from ThermoFisher, 4387406), and RT measured the expression of osteogenic-related genes-qPCR (7500 Fast RT-PCR System, Applied Biosystems®, ThermoFisher Scientific Inc. 4387406). The primers listed in Table II were used for quantification, and GAPDH (FAM®/MGB probe, non-primer limited) (Applied Biosystems®, bought from ThermoFisher, 4333764F)

Table I. $AgNO_3$ concentrations in the cell media for the entirety of the experiment.

Time-point	Base-medium	Control, ppm	0.5, ppm	1.0, ppm	1.5, ppm	TLSN, ppm
Day 0	Complete medium	0.0	0.5	1.0	1.5	0.7
Day 2	Complete medium	0.0	0.5	1.0	1.5	0.7
Day 4	Complete medium	0.0	0.5	1.0	1.5	0.2
Day 6	OIM	0.0	0.5	1.0	1.5	0.2
Day 8	OIM	0.0	0.5	1.0	1.5	0.2
Day 10	OIM	0.0	0.5	1.0	1.5	0.1
Day 12	OIM	0.0	0.5	1.0	1.5	0.1
Day 14	OIM	0.0	0.5	1.0	1.5	0.1
Day 16	OIM	0.0	0.5	1.0	1.5	0.1
Day 18	OIM	0.0	0.5	1.0	1.5	0.1
Day 20	OIM	0.0	0.5	1.0	1.5	0.1
Day 22	OIM	0.0	0.5	1.0	1.5	0.0
Day 24	OIM	0.0	0.5	1.0	1.5	0.0
Day 26	OIM	0.0	0.5	1.0	1.5	0.0

Ppm, parts per million; TLSN, TrabecuLink® with a silver nitrate coating; OIM, osteoinductive cell culture medium.

Table II. TaqMan probes for the primers used in gene expression quantification.

Acronym	Name	TaqMan assay no. ID
COL1A1	Collagen type I alpha 1	Hs00164004_m1
COL1A2	Collagen type I alpha 2	Hs01028970_m1
ALPL	Alkaline phosphatase	Hs01029144_m1

was used as a housekeeping gene. All primers were purchased from ThermoFisher Scientific [TaqMan® Fast Universal PCR Master Mix (2X), catalogue number 4331182, no AmpEras® UNG, product code 4352042]. The melting curves' cycle threshold (CT) values were calculated and expressed using the 2DDΔCT method.

Histochemistry, immunofluorescence, and mineralization assays. Following 4 weeks of culture, the cell nuclei and cytoplasm were stained and visualized with an inverted Leica microscope (Leica DMi8, Microsystem CMS, Wetzlar, Germany) after staining. The cell nuclei were stained with 4',6-diamidino-2-phenylindole (DAPI; Invitrogen, Waltham, MA, USA), and the cytoplasm was stained with carboxyfluorescein diacetate (CFDA; Merck KGaA, Darmstadt, Germany). Intracellular osteocalcin (OCN) was detected by immunofluorescence. In detail, cells were fixed with 4% v/v paraformaldehyde at RT for 20 min and then permeabilized with 0.1% Triton X-100 (Merck KGaA) for 15 min. The cytoplasm was stained with 500 nM CFDA for 15 min. Blocking of unspecific epitopes was performed with a normal 10% goat serum (s-1000; Sigma-Aldrich, Sweden) in a washing solution consisting of PBS with 2% bovine serum albumin (BSA) and 0.3% Triton X-100 for 30 min. The plates were incubated with a solution containing the anti-OCN antibody (20 μg/ml monoclonal mouse anti-human OCN MAB1419; R&D Systems, Abingdon, UK) overnight at 4˚C. The wells were rinsed four times with PBS/1% Triton X-100, and the secondary antibody (1:200, goat anti-mouse, Biotin Novus NB7537; Bio-Techne, Abingdon, UK) was added. The wells were left under agitation at RT. Following the rinsing procedure, the cells were stained with DAPI (300 nM) and Dylight Streptavidin Red (Vector sa-5549, concentration 20 μg/ml), both dissolved in PBS, for a duration of 30 min at RT. Subsequently, the wells were rinsed four times with PBS/1% Triton X-100.

Calcium deposits in the culture wells were measured with Alizarin red staining (AR; Sigma-Aldrich/Merck A5533) as a proxy for mineralization after 4 weeks of culture. The cells were rinsed with PBS and fixed with 70% ice-cold ethanol for 1 h. The wells were then rinsed with distilled water and stained with 40 mM AR at pH 4.2 for 10 min at RT. Next, the dye was removed, and the cells were rinsed with distilled water until the supernatant became transparent, followed by rinsing with PBS on a shaker for 15 min at 300 rpm. The AR dye was finally eluted from the cells with 10 wt% cetylpyridinium chloride (Sigma-Aldrich/Merck C9002) in 10 mM sodium phosphate solution for 20 min at 300 rpm at RT. The absorbance of this supernatant was measured at 562 nm and converted to concentration values ranging from 0.05 to 0.8 mM using an alizarin red calibration curve.

Statistics. All statistical tests were performed using R software version 4.3.3 (24), with the level of statistical significance set at $P<0.05$. To evaluate the difference of the means of the treatment groups at each time point, Levene's test (leveneTest) was used to assess whether the assumption of homogeneity of variance was met before performing an ANOVA (aov). Dunnett's (dunn.test) or Tukey's (TukeyHSD) tests were used for *post hoc* pairwise comparisons, depending on the presence of a control group. If the condition of homogeneity of variance was not met, the nonparametric Kruskal-Wallis test (kruskal.test) was

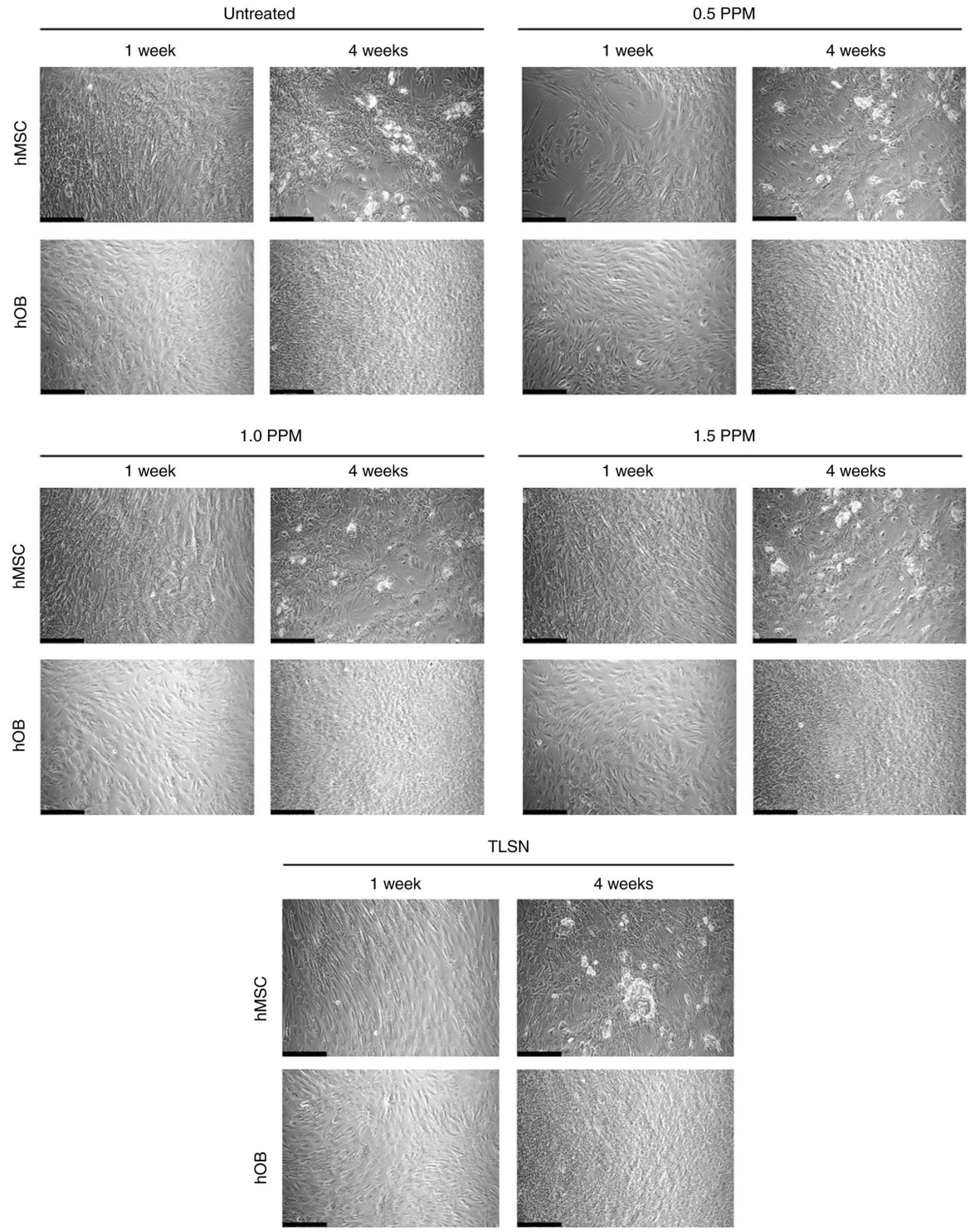

Figure 1. Bright-field microscopy images of hOB and hMSC cultures after 1 and 4 weeks of exposure to various concentrations of Ag^+ in the cell media (scale bar, 280 μm). hMSC, human mesenchymal stem cells; hOB, human osteoblasts; TLSN, simulated Ag^+ release from TrabecuLink with silver nitrate coating.

used with Dunn's test (dunn.test) for pairwise comparisons. Graphs were created with GraphPad Prism, the bar height corresponding to the mean value and the error bars to the standard deviation.

Results

Cell microscopy and immunofluorescence. Both hMSCs and hOBs in the control wells covered the entire area of the well plate and exhibited an elongated fibrillary shape. When visualized with bright-field microscopy after 1 or 4 weeks of culture, no obvious differences were evident in the cell shape or confluence of hMSCs or hOBs after exposure to different Ag^+ concentrations (Fig. 1).

Fluorescence microscopy of fixed and stained cells indicated that hMSCs had a homogenous distribution across the surface of the wells after 4 weeks of culture (Figs. 2, S2), and the cells generally maintained an elongated shape with a

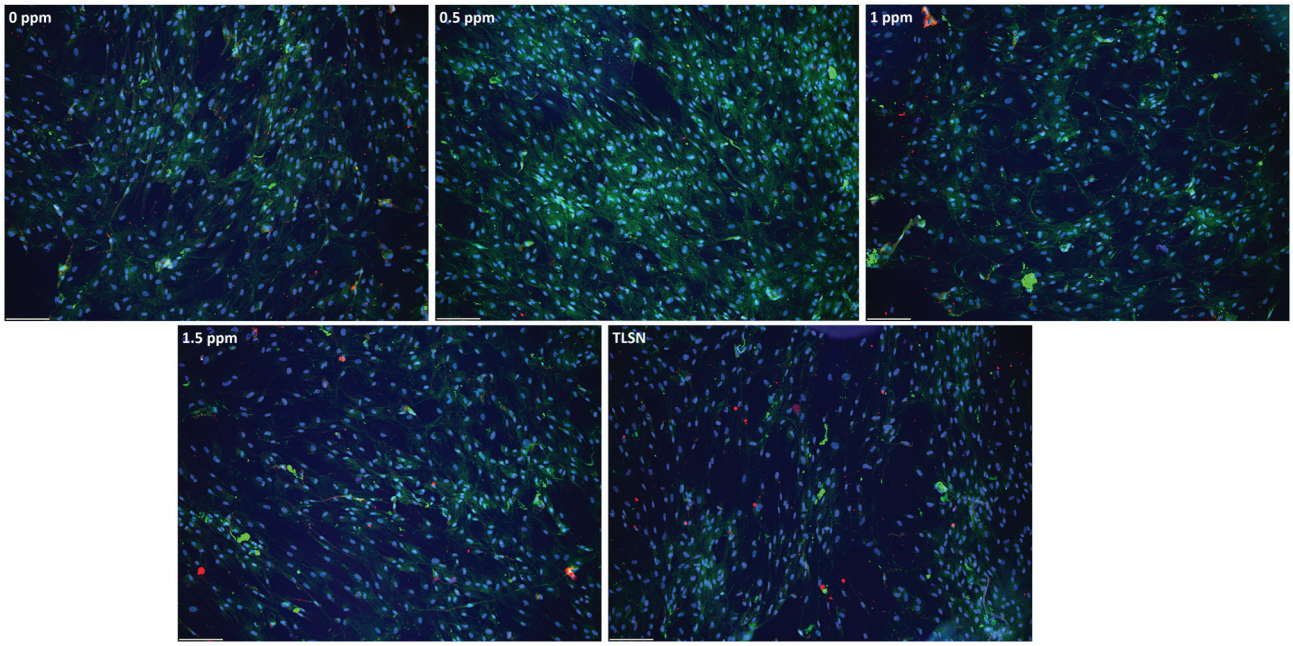

Figure 2. Immunohistochemistry of hMSC cultures after 4 weeks with different concentrations of Ag^+. Blue is DAPI, green is CFDA and red is osteocalcin (scale bar, 140 μm); hMSC, human mesenchymal stem cells; TLSN, simulated Ag^+ release from TrabecuLink with silver nitrate coating.

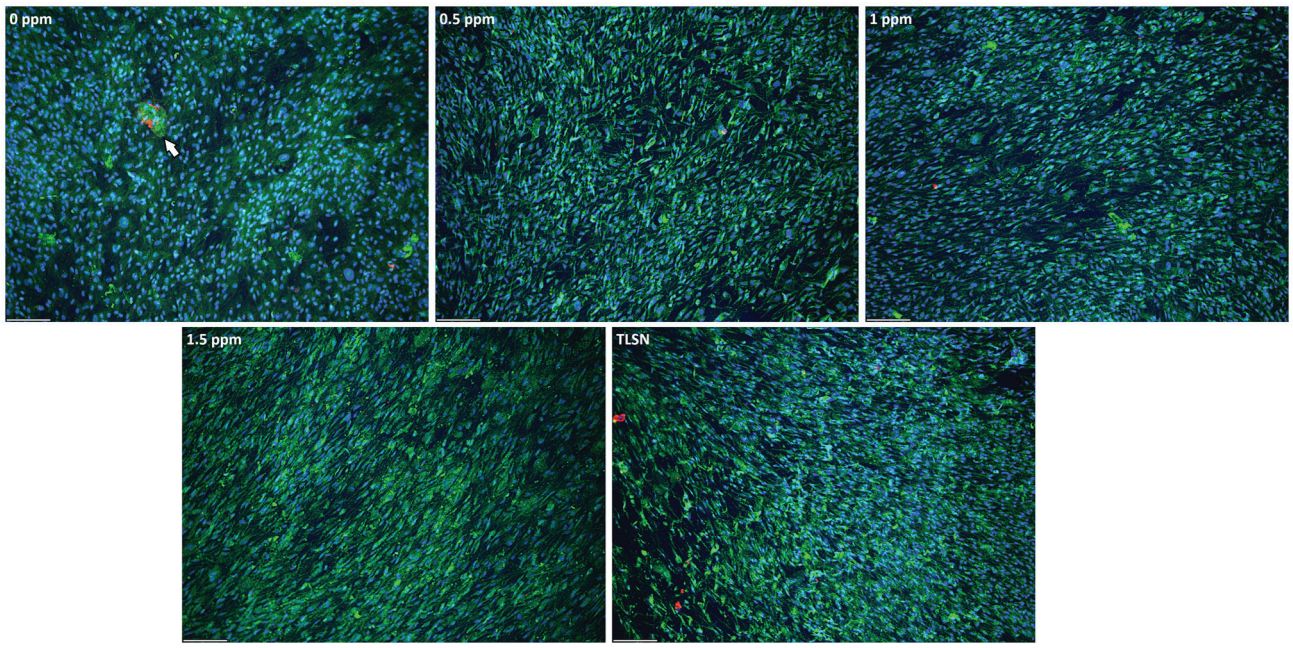

Figure 3. Immunohistochemistry of hOB cultures after 4 weeks with different concentrations of Ag^+; the arrows show an OCN^+ hOB aggregate. Blue is DAPI, green is CFDA and red is osteocalcin (scale bar, 140 μm). hOB, human osteoblasts; TLSN, simulated Ag^+ release from TrabecuLink with silver nitrate coating.

prominent nucleus. Cell growth was slower at an Ag^+ concentration of 1.5 ppm, as evidenced by the sparser cells (Fig. 2). No differences in the OCN staining pattern were detected between cells treated with different Ag^+ concentrations and control cells not exposed to Ag^+ (Figs. 2, S3).

In the untreated hOB cultures, the cells developed a confluent monolayer, exhibiting rapid migration in diverse directions (Fig. 3). Agglomerations of cells, identified by OCN staining, were observed within the untreated group (Figs. 3, S3). With the introduction of Ag^+, no major differences in cell confluence were observed. However, the cellular cytoskeleton of hOB cells exposed to Ag^+ exhibited a thinner profile and a more leaf-shaped morphology. HOBs featured a higher CFDA signal intensity, with a tendency to form aggregates in both the untreated and the Ag^+-exposed groups (Fig. 3). The pattern was similar for all Ag^+ concentrations tested, with no evident OCN staining compared to the untreated group (Fig. S3).

Osteogenic differentiation. In the untreated and Ag-treated hMSC cultures, the ALP/LDH ratio increased with time

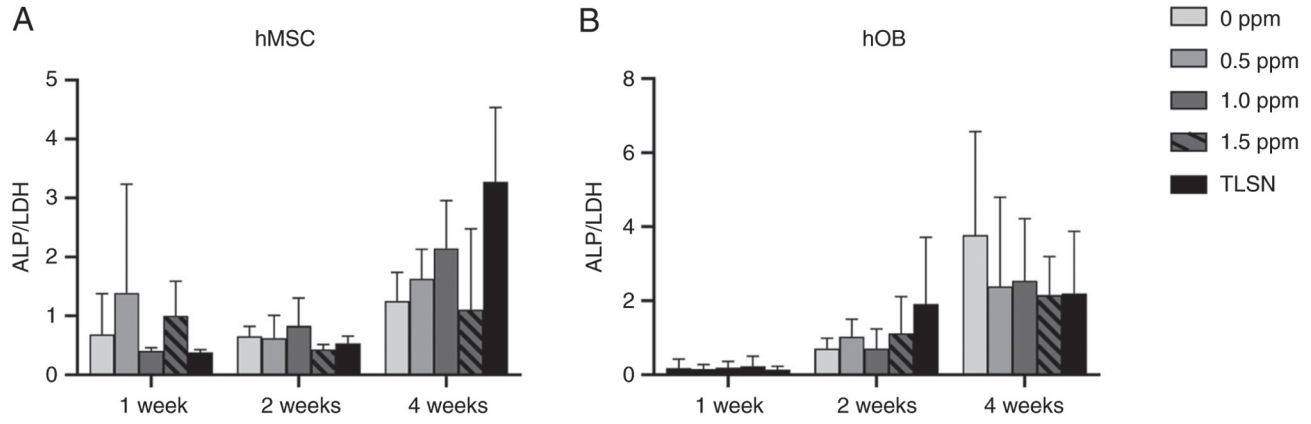

Figure 4. Temporal changes in osteogenic differentiation in (A) hMSC and (B) hOB cultures are expressed as the ratio of ALP to LDH. There were no statistically significant differences between the groups at any given time. The data are expressed as the means ± SDs. ALP, alkaline phosphatase; LDH, lactate dehydrogenase; hMSC, human mesenchymal stem cells; hOB, human osteoblasts; ppm, parts per million; TLSN, simulated Ag^+ release from TrabecuLink with silver nitrate coating.

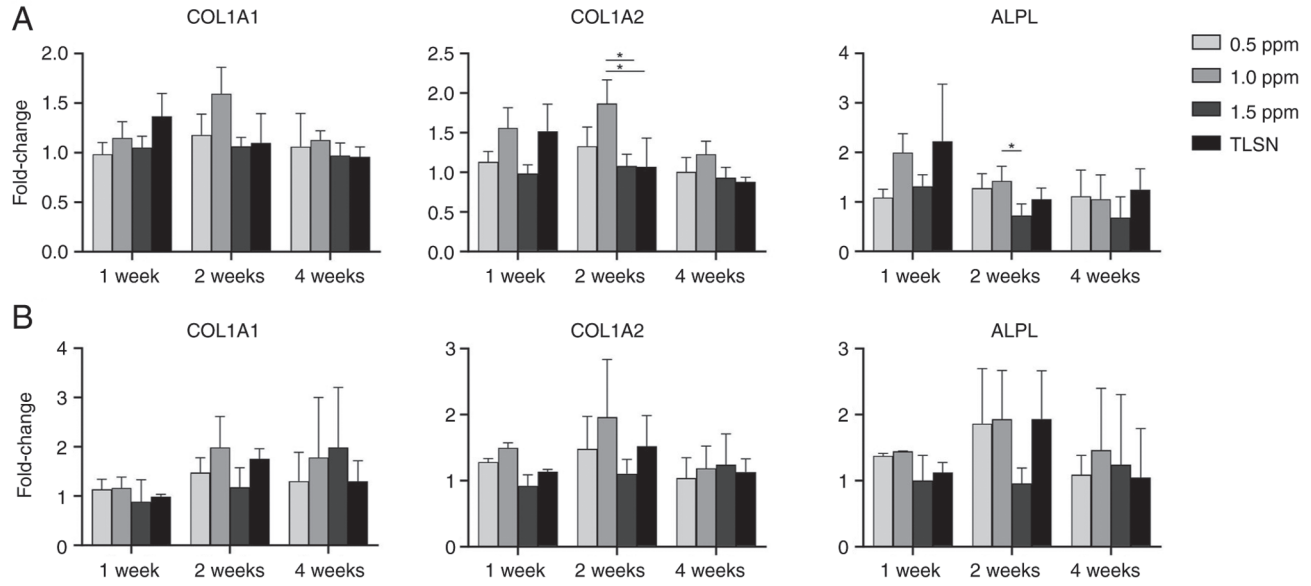

Figure 5. Influence of Ag^+ concentrations on the temporal expression profiles of the COL1A1, COL1A2 and ALPL genes measured by RT-qPCR in (A) hMSC or (B) hOB cultures. The values are expressed as the fold change compared to the control cultures (without adding Ag^+); the data are expressed as the means ± SDs. *P<0.05. hMSC, human mesenchymal stem cells; hOB, human osteoblasts; ppm, parts per million; TLSN, simulated Ag^+ release from TrabecuLink with silver nitrate coating; RT-qPCR, reverse transcription-quantitative PCR.

(Fig. 4), and no statistically significant differences were found between the different Ag^+ concentrations and the control group not exposed to Ag^+ at any time. Overall, the osteogenic activity of the hMSCs was not affected, even at higher concentrations of Ag^+. For the hOBs, the ALP/LDH ratio displayed a more consistent rise, demonstrating a progressive trend over the 4-week period. The highest ratios were observed in the control group not exposed to Ag^+ at the final time point after 4 weeks. In contrast to hMSCs, hOBs were inclined to display decreased osteogenic activity at concentrations of Ag^+ of 0.5 ppm or higher at 4 weeks. However, similar to hMSCs, no statistically significant differences were seen between groups at any time.

Gene expression. In hMSC cultures (Fig. 5A), exposure to Ag^+ concentrations of ≥ 1 ppm significantly suppressed COL1A2 and ALPL gene transcription after 2 weeks of culture. Gene expression showed an upward trend during the first week of culture but then gradually decreased over time. In hOB cultures, no clear concentration-dependent effect was detected (Fig. 5B). In hOB cells at 4 weeks, the genes did not generally display a clear pattern of change with increasing concentrations of Ag^+. Gene expression trended upward over time without significant differences between Ag^+ concentrations.

Cell mineralization. Robust mineralization was detected in hMSCs cultured in control media after 4 weeks of culture (Figs. 6A, S1). However, the alizarin red staining intensity showed a decreasing trend with increasing Ag^+ concentration, and the lowest signal was found at 1.5 ppm; however, no statistically significant differences were found. In hOB, on the other hand (Fig. 6B), a statistically significant reduction in mineralization was observed for Ag^+ concentrations ≥1 ppm

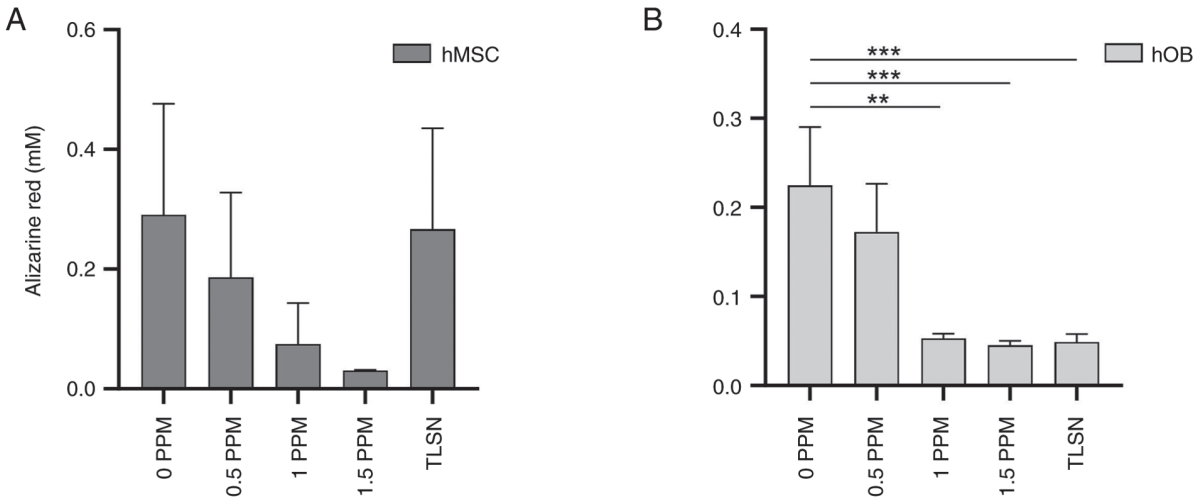

Figure 6. Alizarin red concentration in the wells after 4 weeks of (A) hMSC and (B) hOB culture. The data are expressed as the means ± SDs. **P=0.01, ***P<0.001. hMSC, human mesenchymal stem cells; hOB, human osteoblasts; ppm, parts per million; TLSN, simulated Ag^+ release from TrabecuLink with silver nitrate coating.

compared to that in the control group not exposed to Ag^+. These findings indicated that osteoid deposition in hOB was severely hampered at concentrations of ≥1 ppm.

Discussion

This study examined the effects of different Ag^+ concentrations on the viability, osteogenic differentiation, osteogenic gene expression, and mineralization of hMSC and hOB cultures. We found that matrix mineralization in hOBs was notably reduced at higher concentrations of Ag^+, particularly at concentrations >1 ppm, indicating a negative impact on mineralization by these cells. However, after 4 weeks of culture, no cell shape or confluence differences were discernible between media containing varying Ag^+ concentrations when examined using bright field microscopy. HOBs, however, which is a slower proliferative cell type than hMSCs, featured a higher CFDA signal intensity. No significant differences were observed in ALP/LDH ratios between hMSC and hOB cultures exposed to varying Ag^+ concentrations over time. A trend was observed in the hOB cultures at 4 weeks, showing a lower ALP/LDH ratio with an increasing Ag^+ concentration. The osteogenic genes ALPL, COL1A1, and COL1A2 expression tended to decrease with Ag^+ concentrations >1 ppm in both hMSCs and hOBs. However, no clear concentration-dependent response was detected, with statistically significant effects only being detected in hMSCs.

The impact of Ag exposure on hMSC cultures is variable and contingent upon culture conditions and Ag concentrations (25-27). For example, Ag^+ exposure of hMSCs (approximately 3 ppm) for up to 3 weeks in a spheroid culture has been shown to increase osteogenic gene expression through WNT and MAPK signaling without impacting matrix mineralization (26). Alternatively, Ag-induced oxidative stress might induce adipogenesis in hMSCs (27). Our study demonstrated statistically significant differences in the expression of osteogenic genes in hMSCs treated with increasing Ag^+ concentrations, as well as a trend toward decreased mineralization. It has been suggested that Ag^+ in the range of 0.1 to 1.6 ppm preserves the antibacterial properties of Ag and prevents toxicity to osteogenic cells (28,29). A previous study conducted by our research group (6), showed that hOBs cultured on 3D-printed, Ag-coated trabecular titanium discs (TLSN) and exposed to a cumulative release of 3.5 ppm after 4 weeks did not express significant differences in ALP production or overall viability compared to cells cultured on uncoated control discs. While hMSC cultures exhibited an increasing trend in osteogenic marker expression over the first week, followed by a gradual decrease, hOB cultures tended to increase osteogenic marker expression. This increase may be attributable to the maturity of the hOB expressing these markers. However, compared to the uncoated controls, we noted a trend for downregulating the COL1A1 and COL1A2 genes in hOB at 4 weeks and an upregulation of ALPL. The decreased gene expression observed at 4 weeks relative to 2 weeks could be attributed to contact inhibition among the cells. Previous research conducted by our group, involving the culture of hOB on TLSN implants, revealed a tendency towards decreased mineralization. However, statistically significant differences were not observed compared to cells cultured on non-silver-coated implants (6). Nevertheless, it is noteworthy that the TLSN implants used as substrates for the cell cultures in those experiments had an average roughness of Ra=5.0 μm. This factor may have improved the osteogenic cell response despite exposure to Ag^+ (6,30). Ag-coated implants possessing distinct physicochemical properties conducive to osteogenic cell adhesion, proliferation, and differentiation might mitigate the cytotoxic effects of Ag. This cytotoxic effect would be more pronounced when cells are solely exposed to Ag^+ and cultured on a smooth, less supportive substrate compared to trabecular titanium. Examples of modifications supporting osteogenic cells include specific surface geometries (31,32) and the use of composite materials, such as those containing Sr (33,34), Ga (35) or hydroxyapatite (8,36). Another parameter contributing to the discrepancy between our findings and those documented in previous works is that Ag^+ in nanoparticle form may be less cytotoxic than Ag^+ in an aqueous solution, as in the $AgNO_3$ solutions used in our current experiments (37).

Our study did not observe any differences in the gene expression of hOB for the examined range of Ag^+ concentrations. However, osteoid deposition was adversely affected at concentrations ≥1 ppm, suggesting that these levels could compromise implant stability when employed in a press-fit application. This disparity in the mineralization data in comparison to our previous study (6) might be attributed to the inherent variability that hOBs exhibit from patient to patient.

One of the strengths of our study is the use of not only commercially available hMSCs but also patient-derived primary hOBs. In contrast, many other studies in Ag and osseointegration use only commercially accessible cells or cell lines (38). HMSCs are a widely employed and relevant cell type; however, the less frequently used hOB can more closely mimic clinical conditions (39). A limitation of hOBs is their greater biological variation, as they differ from patient to patient. For this study's experiments, hOBs from up to five patients were used. An additional strength of our study lies in its use of diverse modalities for evaluating osteogenic differentiation, encompassing morphological cell analysis, ALP measurements, LDH enzymatic activity, a comprehensive panel of osteogenic genes, and a mineralization assay. Long-term cultures, lasting up to 4 weeks, were used and are preferable to short-term experiments (25-28) in discerning the effects of chronic Ag^+ exposure and facilitating investigations into the slower mineralization processes. Future research should explore the effects of a more restricted range of Ag^+ concentrations on a broader spectrum of osteogenic genes, encompassing Runx2, osteonectin, osteopontin, and osteocalcin.

Although the future looks promising for some Ag-coated implants, such as plates (15), nails (13), and cemented megaprostheses (2), the question of Ag-coated press-fit hip stems persists. Stability is achieved in the press-fit concept when the implant transitions from primary stability to secondary stability by osseointegration, which occurs through mineralization and bone remodeling, eliminating micromotions. Reduced mineralization can lead to long-term implant loosening due to sustained micromotion. For press-fit implants featuring antibacterial coatings, minimizing toxicity towards osteoblasts is paramount (5,40). *In vitro* experiments offer a rough estimate of how cells react to specific antibacterial coatings. Still, *in vivo* experiments are mandatory because they can offer biomechanical (41) and histological data on osseointegration and bone formation around coated implants. Our study lacks these important data (40). Overall, Ag coating is an effective strategy for reducing infection rates (2). However, providing clinical recommendations requires robust, randomized, controlled trials. For example, the BASICS (42), a multicenter randomized trial, showed that Ag-coated ventriculoperitoneal shunts did not perform better than uncoated shunts in reducing infection rates. However, such studies do not exist in orthopedic surgery. The hOB experiments constitute a more valid model than those using hMSCs, as hOBs are sourced from the femoral head of human donors and more closely replicate the cell types that would interact with an Ag^+-coated implant. Chronic Ag^+ release from the implant into the periprosthetic space, and consequently through tissue continuity to the bone, potentially hinders osteoblast activity and bone formation, as seen in our hOB experiments. Over time, this process may reduce bone apposition around the implant. Therefore, we recommend limiting Ag^+ release from the implant both in its concentration and duration of exposure.

The supplementation of Ag^+ in the growth medium of hMSC and hOB cultures over 4 weeks did not confer any differences in cell viability and differentiation. Still, statistically significant differences were noted in the expression of the osteogenic genes COL1A2 and ALPL in hMSC cultures. The presence of Ag^+ in the hMSC culture medium, mimicking the release profile of TLSN implants, did not impact mineralization. However, mineralization was profoundly compromised in hOB cultures. This observation underscores the importance of accounting for cell type-specific responses when evaluating the biocompatibility of implant compounds, such as Ag, given that the effects on hOBs are likely more representative of the actual *in vivo* scenario. If the implant is designed for uncemented fixation within the host bone, a thorough investigation of the Ag^+ release profile from the implant and its associated cellular responses is crucial.

Acknowledgements

Not applicable.

Funding

The study was funded by grants from the Swedish Research Council (grant no. VR 2021-00980) and Stiftelsen Promobilia (grant no. A23003).

Availability of data and materials

The data generated in the present study may be requested from the corresponding author.

Authors' contributions

MGK analyzed and curated the data, performed the experiments, wrote, reviewed and edited the original draft, and created the figures. EC performed the experiments, curated the data and reviewed and editing the manuscript. CPN validated the reproducibility of the experiments, contributed to the analysis and interpretation of data, supervised the study and reviewed and edited the manuscript. NPH conceptualized and supervised the study, designed the methodology, validated the reproducibility of the experiments, reviewed and edited the manuscript and acquired funding. MGK, EC and CPN confirm the authenticity of all raw data. All authors read and approved the final manuscript.

Ethics approval and consent to participate

This study was approved by the Swedish Ethical Review Authority (approval no. 2020-04462).

Patient consent for publication

Patient consent was waived for this study based on section 4, subsection 3 of the relevant law (2003:460) which specifies that the requirement for informed consent applies only when biological material collected from patients can be traced back

to the individual patient. This was confirmed by the above ethics committee, as the hOBs used in this study are not traceable to specific patients.

Competing interests

Michael G. Kontakis, Elin Carlsson and Carlos Palo-Nieto declare that they have no competing interests. Nils P. Hailer reports receiving institutional support and lecturer honoraria from two hip implant manufacturers, Waldemar Link GmbH & Co. KG and Zimmer Biomet, as well as lecturer honoraria from Heraeus, a bone cement manufacturer.

References

1. Wyatt MC, Foxall-Smith M, Roberton A, Beswick A, Kieser DC and Whitehouse MR: The use of silver coating in hip megaprostheses: A systematic review. HIP Int 29: 7-20, 2019.
2. Hardes J, Henrichs MP, Hauschild G, Nottrott M, Guder W and Streitbuerger A: Silver-Coated megaprosthesis of the proximal tibia in patients with sarcoma. J Arthroplasty 32: 2208-2213, 2017.
3. Fiore M, Sambri A, Zucchini R, Giannini C, Donati DM and De Paolis M: Silver-coated megaprosthesis in prevention and treatment of peri-prosthetic infections: A systematic review and meta-analysis about efficacy and toxicity in primary and revision surgery. Eur J Orthop Surg Traumatol 31: 201-220, 2021.
4. Sportelli MC, Izzi M, Volpe A, Clemente M, Picca RA, Ancona A, Lugarà PM, Palazzo G and Cioffi N: The pros and cons of the use of laser ablation synthesis for the production of silver nano-antimicrobials. Antibiotics (Basel) 7: 67, 2018.
5. Kontakis MG, Diez-Escudero A, Hariri H, Andersson B, Jarhult JD and Hailer NP: Antimicrobial and osteoconductive properties of two different types of titanium silver coating. Eur Cell Mater 41: 694-706, 2021.
6. Diez-Escudero A, Andersson B, Carlsson E, Recker B, Link H, Jarhult JD and Hailer NP: 3D-printed porous Ti6Al4V alloys with silver coating combine osteocompatibility and antimicrobial properties. Biomater Adv 133: 112629, 2022.
7. Morimoto T, Hirata H, Eto S, Hashimoto A, Kii S, Kobayashi T, Tsukamoto M, Yoshihara T, Toda Y and Mawatari M: Development of silver-containing hydroxyapatite-coated antimicrobial implants for orthopaedic and spinal surgery. Medicina (Kaunas) 58: 519, 2022.
8. Eto S, Kawano S, Someya S, Miyamoto H, Sonohata M and Mawatari M: First clinical experience with thermal-sprayed silver oxide-containing hydroxyapatite coating implant. J Arthroplasty 31: 1498-1503, 2016.
9. Diez-Escudero A and Hailer NP: The role of silver coating for arthroplasty components. Bone Joint J 103-B: 423-429, 2021.
10. Glehr M, Leithner A, Friesenbichler J, Goessler W, Avian A, Andreou D, Maurer-Ertl W, Windhager R and Tunn PU: Argyria following the use of silver-coated megaprostheses. Bone Joint J 95-B: 988-992, 2013.
11. Hardes J, Ahrens H, Gebert C, Streitbuerger A, Buerger H, Erren M, Gunsel A, Wedemeyer C, Saxler G, Winkelmann W and Gosheger G: Lack of toxicological side-effects in silver-coated megaprostheses in humans. Biomaterials 28: 2869-2875, 2007.
12. Hussmann B, Johann I, Kauther MD, Landgraeber S, Jäger M and Lendemans S: Measurement of the silver ion concentration in wound fluids after implantation of silver-coated megaprostheses: Correlation with the clinical outcome. Biomed Res Int 2013: 1-11, 2013.
13. Karupiah T, Yong AP, Ong ZW, Tan HK, Tang WC and Salam HB: Use of a novel anti-infective noble metal alloy-coated titanium orthopedic nail in patients with open fractures: A case series from Malaysia. Antibiotics (Basel) 11: 1763, 2022.
14. Schoder S, Lafuente M and Alt V: Silver-coated versus uncoated locking plates in subjects with fractures of the distal tibia: A randomized, subject and observer-blinded, multi-center non-inferiority study. Trials 23: 968, 2022.
15. Arens D, Zeiter S, Nehrbass D, Ranjan N, Paulin T and Alt V: Antimicrobial silver-coating for locking plates shows uneventful osteotomy healing and good biocompatibility results of an experimental study in rabbits. Injury 51: 830-839, 2020.
16. Shimabukuro M, Tsutsumi Y, Yamada R, Ashida M, Chen P, Doi H, Nozaki K, Nagai A and Hanawa T: Investigation of realizing both antibacterial property and osteogenic cell compatibility on titanium surface by simple electrochemical treatment. ACS Biomater Sci Eng 5: 5623-5630, 2019.
17. Komori T: Regulation of bone development and extracellular matrix protein genes by RUNX2. Cell Tissue Res 339: 189-195, 2010.
18. Choi KY, Lee SW, Park MH, Bae YC, Shin HI, Nam S, Kim YJ, Kim HJ and Ryoo HM: Spatio-temporal expression patterns of Runx2 isoforms in early skeletogenesis. Exp Mol Med 34: 426-433, 2002.
19. Hauschka PV, Lian JB, Cole DE and Gundberg CM: Osteocalcin and matrix Gla protein: Vitamin K-dependent proteins in bone. Physiol Rev 69: 990-1047, 1989.
20. Jayakumar P and Di Silvio L: Osteoblasts in bone tissue engineering. Proc Inst Mech Eng H 224: 1415-1440, 2010.
21. Mestres G, Carter SD, Hailer NP and Diez-Escudero A: A practical guide for evaluating the osteoimmunomodulatory properties of biomaterials. Acta Biomater 130: 115-137, 2021.
22. Grzeskowiak RM, Schumacher J, Dhar MS, Harper DP, Mulon PY and Anderson DE: Bone and cartilage interfaces with orthopedic implants: A literature review. Front Surg 7: 601244, 2020.
23. Dillon JP, Waring-Green VJ, Taylor AM, Wilson PJM, Birch M, Gartland A and Gallagher JA: Primary human osteoblast cultures. Methods Mol Biol 816: 3-18, 2012.
24. R Core Team (2021). R: A language and environment for statistical computing. R Foundation for Statistical Computing, Vienna, Austria. URL https://www.R-project.org/.
25. Liu X, He W, Fang Z, Kienzle A and Feng Q: Influence of silver nanoparticles on osteogenic differentiation of human mesenchymal stem cells. J Biomed Nanotechnol 10: 1277-1285, 2014.
26. Kersey AL, Singh I and Gaharwar AK: Inorganic ions activate lineage-specific gene regulatory networks. Acta Biomater 183: 371-386, 2024.
27. He W, Elkhooly TA, Liu X, Cavallaro A, Taheri S, Vasilev K and Feng Q: Silver nanoparticle-based coatings enhance adipogenesis compared to osteogenesis in human mesenchymal stem cells through oxidative stress. J Mater Chem B 4: 1466-1479, 2016.
28. Saravanapavan P, Gough JE, Jones JR and Hench LL: Antimicrobial macroporous gel-glasses: Dissolution and cytotoxicity. Key Engineering Materials 254-256: 1087-1090, 2003.
29. Panacek A, Kvitek L, Prucek R, Kolar M, Vecerova R, Pizurova N, Sharma VK, Nevecna T and Zboril R: Silver colloid nanoparticles: Synthesis, characterization, and their antibacterial activity. J Phys Chem B 110: 16248-16253, 2006.
30. Feller L, Jadwat Y, Khammissa RAG, Meyerov R, Schechter I and Lemmer J: Cellular responses evoked by different surface characteristics of intraosseous titanium implants. Biomed Res Int 2015: 171945, 2015.
31. Diez-Escudero A, Andersson B, Persson C and Hailer NP: Hexagonal pore geometry and the presence of hydroxyapatite enhance deposition of mineralized bone matrix on additively manufactured polylactic acid scaffolds. Mater Sci Eng C Mater Biol Appl 125: 112091, 2021.
32. Sanchez-Salcedo S, Garcia A, Gonzalez-Jimenez A and Vallet-Regi M: Antibacterial effect of 3D printed mesoporous bioactive glass scaffolds doped with metallic silver nanoparticles. Acta Biomater 155: 654-666, 2023.
33. Parizi MK, Doll K, Rahim MI, Mikolai C, Winkel A and Stiesch M: Antibacterial and cytocompatible: Combining silver nitrate with strontium acetate increases the therapeutic window. Int J Mol Sci 23: 8058, 2022.
34. Cheng H, Xiong W, Fang Z, Guan H, Wu W, Li Y, Zhang Y, Alvarez MM, Gao B, Huo K, *et al*: Strontium (Sr) and silver (Ag) loaded nanotubular structures with combined osteoinductive and antimicrobial activities. Acta Biomater 31: 388-400, 2016.
35. Pinera-Avellaneda D, Buxadera-Palomero J, Delint RC, Dalby MJ, Burgess KV, Ginebra MP, Rupérez E and Manero JM: Gallium and silver-doped titanium surfaces provide enhanced osteogenesis, reduce bone resorption and prevent bacterial infection in co-culture. Acta Biomater 180: 154-170, 2024.
36. Eto S, Miyamoto H, Shobuike T, Noda I, Akiyama T, Tsukamoto M, Ueno M, Someya S, Kawano S, Sonohata M and Mawatari M: Silver oxide-containing hydroxyapatite coating supports osteoblast function and enhances implant anchorage strength in rat femur. J Orthop Res 33: 1391-1397, 2015.
37. Yusuf A and Casey A: Liposomal encapsulation of silver nanoparticles (AgNP) improved nanoparticle uptake and induced redox imbalance to activate caspase-dependent apoptosis. Apoptosis 25: 120-134, 2020.

38. Spriano S, Yamaguchi S, Baino F and Ferraris S: A critical review of multifunctional titanium surfaces: New frontiers for improving osseointegration and host response, avoiding bacteria contamination. Acta Biomater 79: 1-22, 2018.
39. Czekanska EM, Stoddart MJ, Richards RG and Hayes JS: In search of an osteoblast cell model for in vitro research. Eur Cells Mater 24: 1-17, 2012.
40. Bretschneider H, Mettelsiefen J, Rentsch C, Gelinsky M, Link HD, Gunther KP, Lode A and Hofbauer C: Evaluation of topographical and chemical modified TiAl6V4 implant surfaces in a weight-bearing intramedullary femur model in rabbit. J Biomed Mater Res B Appl Biomater 108: 1117-1128, 2020.
41. Hauschild G, Hardes J, Gosheger G, Stoeppeler S, Ahrens H, Blaske F, Wehe C, Karst U and Höll S: Evaluation of osseous integration of PVD-silver-coated hip prostheses in a canine model. Biomed Res Int 2015: 292406, 2015.
42. Mallucci CL, Jenkinson MD, Conroy EJ, Hartley JC, Brown M, Dalton J, Kearns T, Moitt T, Griffiths MJ, Culeddu G, *et al*: Antibiotic or silver versus standard ventriculoperitoneal shunts (BASICS): A multicentre, single-blinded, randomised trial and economic evaluation. Lancet 394: 1530-1539, 2019.